

Logarithmic landscape and power-law escape rate of SGD

Takashi Mori¹, Liu Ziyin², Kangqiao Liu², and Masahito Ueda^{2,1,3}

¹*RIKEN Center for Emergent Matter Science (CEMS), Wako, Saitama 351-0198, Japan*

²*Department of Physics, The University of Tokyo, Bunkyo-ku, Tokyo 113-0033, Japan*

³*Institute for Physics of Intelligence, The University of Tokyo, Bunkyo-ku, Tokyo 113-0033, Japan*

Stochastic gradient descent (SGD) undergoes complicated multiplicative noise for the mean-square loss. We use this property of the SGD noise to derive a stochastic differential equation (SDE) with simpler additive noise by performing a non-uniform transformation of the time variable. In the SDE, the gradient of the loss is replaced by that of the logarithmized loss. Consequently, we show that, near a local or global minimum, the stationary distribution $P_{ss}(\theta)$ of the network parameters θ follows a power-law with respect to the loss function $L(\theta)$, i.e. $P_{ss}(\theta) \propto L(\theta)^{-\phi}$ with the exponent ϕ specified by the mini-batch size, the learning rate, and the Hessian at the minimum. We obtain the escape rate formula from a local minimum, which is determined not by the loss barrier height $\Delta L = L(\theta^s) - L(\theta^*)$ between a minimum θ^* and a saddle θ^s but by the logarithmized loss barrier height $\Delta \log L = \log[L(\theta^s)/L(\theta^*)]$. Our escape-rate formula explains an empirical fact that SGD prefers flat minima with low effective dimensions.

1 Introduction

Deep learning has achieved breakthroughs in various applications in artificial intelligence such as image classification [1, 2], speech recognition [3], natural language processing [4], and natural science [5–7]. Such unparalleled success of deep learning hinges crucially on stochastic gradient descent (SGD) or its variants as an efficient algorithm for training deep neural networks.

Although the loss landscape is highly nonconvex, the SGD often succeeds in finding a global minimum. It has been argued that the SGD noise plays a key role in escaping from local minima [8–14]. It has also been suggested that SGD is beneficial for generalization.

That is, SGD may help the network to find *flat minima*, which are considered to imply good generalization [9, 15, 16].

How and why does SGD help the network escape from bad local minima and find flat minima? These questions have been addressed in several works, and it is now recognized that the SGD noise strength and structure importantly affect the efficiency of escape from local minima. Our work follows this line of research, and add new theoretical perspectives.

In physics and chemistry, escape from a local minimum of the (free) energy landscape due to thermal noise at temperature T has been thoroughly discussed [17, 18]. When the (free) energy barrier is given by ΔE , the escape rate is proportional to $e^{-\Delta E/T}$, which is known as the Arrhenius law. By analogy, in machine learning, escape from a local minimum of the loss function is considered to be determined by the loss barrier height $\Delta L = L(\theta^s) - L(\theta^*)$, where $L(\theta)$ denotes the loss function at the network parameters θ , θ^* stands for a local minimum of $L(\theta)$, and θ^s denotes a saddle point that separates θ^* from other minima. If we assume that the SGD noise is uniform and isotropic, which is often assumed in machine-learning literature [8], the escape rate is proportional to $e^{-\Delta L/D}$, where D denotes the SGD noise strength. Recent studies take some structure of the SGD noise into account, but the escape rate derived so far is determined by the loss barrier height ΔL [11–14].

In this paper, we show that the inhomogeneity of the SGD noise strength brings about drastic modification for the mean-square loss. In particular, it turns out that the escape rate is determined by the *logarithmized* loss barrier height $\Delta \log L = \log L(\theta^s) - \log L(\theta^*) = \log[L(\theta^s)/L(\theta^*)]$. In other words, the escape rate is determined by not the difference but the ratio of $L(\theta^s)$ and $L(\theta^*)$. This observation implies the importance of examining the landscape of $\log L(\theta)$, which is a new theoretical observation brought into the study of the SGD dynamics.

The above result is derived by the following property of the SGD noise: the SGD noise is stronger when the loss is larger. Indeed, for the mean-square loss, we show that the SGD noise strength at θ is proportional to $L(\theta)$. Our formula on the escape rate implies that SGD prefers minima at which (i) the “effective dimension” [19] is small, i.e., a bulk of the eigenvalues of the Hessian of the loss function are concentrated near zero and (ii) typical values of other eigenvalues are also small. The property (ii) implies that minima are flat. The property (i) is less intuitive but consistent with the spectral analysis of the Hessian for trained networks, which reveals that the Hessian eigenvalues are separated into two groups: a bulk of almost zero eigenvalues and a small number of outliers [20, 21]. Our theory explains these empirical observations.

Main contributions: In summary, we obtain the following main results:

- The SGD noise strength in the mean-square loss strongly depends on the position in the parameter space and is proportional to the loss function [see Eq. (14)]. This result is derived theoretically and also confirmed experimentally (see Sec. 5.2).
- The derived SGD noise covariance structure implies the importance of the logarithmized loss landscape. Specifically, by introducing the non-uniform transformation

of time variable, we derive the Langevin equation with additive noise, in which the loss gradient is replaced by the logarithmized loss gradient. Its stationary distribution follows the power law with respect to the loss function.

- Consequently, the escape rate from a local minimum is governed by the logarithmized loss barrier height [see Eqs. (22) and (27)], and significantly depends on the effective dimension of a local minimum. A local minimum with a larger effective dimension is more unstable.

Related works: The role of the SGD noise structure has been discussed in some previous works [11–14]. Remarkably, it was pointed out that the anisotropic nature of the SGD noise is important: the SGD noise is aligned with the Hessian of the loss function near minima, which is beneficial for escape from sharp minima [11–13]. The anisotropy of the SGD noise also plays an important role in our work: due to it, the SGD dynamics is frozen along flat directions of the loss function. Compared with the anisotropy of the SGD noise, the inhomogeneity of the SGD noise strength has been less explored. An exception is the work by Meng *et al.* [14], where the SGD dynamics under a state-dependent noise is discussed. However, in Ref. [14], the connection between the noise strength and the loss function was not theoretically established, and the logarithmized loss landscape was not discussed. Our escape rate (27) depends polynomially on the ratio of the losses at a minimum and a saddle rather than exponentially on the difference of the two as in formulae derived in the previous works [11–13], in which the inhomogeneity of the noise strength is not taken into account.

2 Background

2.1 Setup

We consider supervised learning. Let $\mathcal{D} \{(x^{(\mu)}, y^{(\mu)}) : \mu = 1, 2, \dots, N\}$ be the training dataset, where $x^{(\mu)} \in \mathbb{R}^d$ denotes a data vector and $y^{(\mu)} \in \mathbb{R}$ be its label. The network output for a given input x is denoted by $f(\theta, x) \in \mathbb{R}$, where $\theta \in \mathbb{R}^P$ stands for a set of trainable parameters with P being the number of trainable parameters.¹ In this work, we focus on the mean-square loss

$$L(\theta) = \frac{1}{2N} \sum_{\mu=1}^N \left[f(\theta, x^{(\mu)}) - y^{(\mu)} \right]^2 =: \frac{1}{N} \sum_{\mu=1}^N \ell_{\mu}(\theta). \quad (1)$$

The training proceeds through optimization of $L(\theta)$. In most machine-learning applications, the optimization is done via SGD or its variants. In SGD, the parameter θ_{k+1} at the time step $k + 1$ is determined by

$$\theta_{k+1} = \theta_k - \eta \nabla L_{B_k}(\theta_k), \quad L_{B_k}(\theta) = \frac{1}{2B} \sum_{\mu \in B_k} \ell_{\mu}(\theta), \quad (2)$$

¹Extension to the multi-dimensional output $f(\theta, x) \in \mathbb{R}^m$ is straightforward.

where $\eta > 0$ is the learning rate, $B_k \subset \{1, 2, \dots, N\}$ with $|B_k| = B$ is a mini-batch used at the k th time step, and L_{B_k} denotes the mini-batch loss.

Since the training dataset \mathcal{D} is randomly divided into mini-batches, the dynamics defined by Eq. (2) is stochastic. When $B = N$, the full training data samples are used for every iteration. In this case, the dynamics is deterministic and called gradient descent (GD). SGD is interpreted as GD with stochastic noise. By introducing the SGD noise $\xi_k = -[\nabla L_{B_k}(\theta_k) - \nabla L(\theta_k)]$, Eq. (2) is rewritten as

$$\theta_{k+1} = \theta_k - \eta \nabla L(\theta_k) + \eta \xi_k. \quad (3)$$

Obviously, $\langle \xi_k \rangle = 0$, where the brackets denote the average over possible choices of mini-batches. The noise covariance matrix is defined as $\Sigma(\theta_k) := \langle \xi_k \xi_k^T \rangle$. The covariance structure of the SGD noise is important in analyzing the SGD dynamics, which will be discussed in Sec. 3.1.

2.2 Stochastic differential equation for SGD

When the parameter update for each iteration is small, which is typically the case when the learning rate η is small enough, we can consider the continuous-time approximation [22, 23]. By introducing a continuous time variable $t \in \mathbb{R}$ and regarding η as an infinitesimal time step dt , we have the stochastic differential equation

$$d\theta_t = -\nabla L(\theta_t)dt + \sqrt{\eta \Sigma(\theta_t)} \cdot dW_t, \quad (4)$$

where $dW_t \sim \mathcal{N}(0, I_P dt)$ with I_n being the n -by- n identity matrix, and the multiplicative noise $\sqrt{\eta \Sigma(\theta_t)} \cdot dW_t$ is interpreted as Itô since the noise ξ_k in Eq. (3) depends on θ_k but not on θ_{k+1} . Throughout this work, we consider the continuous-time approximation (4) with Gaussian noise.

In machine learning, the gradient Langevin dynamics (GLD) is also considered, in which the isotropic and uniform Gaussian noise is injected into the GD as

$$d\theta_t = -\nabla L(\theta_t)dt + \sqrt{2D}dW_t, \quad (5)$$

where $D > 0$ corresponds to the noise strength (it is also called the diffusion coefficient) [11, 24, 25]. The stationary probability distribution $P_{\text{GLD}}(\theta)$ of θ for GLD is given by the Gibbs distribution

$$P_{\text{GLD}}(\theta) = \frac{1}{Z_{\text{GLD}}} e^{-L(\theta)/D}, \quad Z_{\text{GLD}} = \int d\theta e^{-L(\theta)/D}. \quad (6)$$

We will see in Sec. 4 that the SGD noise structure, which is characterized by $\Sigma(\theta)$, drastically alters the stationary distribution.

3 Theoretical formulation

3.1 Structure of the SGD noise covariance

The SGD noise covariance matrix $\Sigma(\theta)$ significantly affects the dynamics. Here we summarize some important properties of $\Sigma(\theta)$. First, we start from an analytic expression

of $\Sigma(\theta)$, which reads

$$\Sigma(\theta) = \frac{1}{B} \frac{N-B}{N-1} \left(\frac{1}{N} \sum_{\mu=1}^N \nabla \ell_{\mu} \nabla \ell_{\mu}^T - \nabla L \nabla L^T \right) \simeq \frac{1}{B} \left(\frac{1}{N} \sum_{\mu=1}^N \nabla \ell_{\mu} \nabla \ell_{\mu}^T - \nabla L \nabla L^T \right), \quad (7)$$

where $B \ll N$ is assumed in the second equality. The derivation of Eq. (7) is found in [8, 23]. Usually, the gradient noise variance dominates the square of the gradient noise mean, and hence the term $\nabla L \nabla L^T$ in Eq. (7) is negligible. We therefore obtain

$$\Sigma(\theta) \simeq \frac{1}{BN} \sum_{\mu=1}^N \nabla \ell_{\mu} \nabla \ell_{\mu}^T. \quad (8)$$

For the mean-square loss, we have $\nabla \ell_{\mu} = [f(\theta, x^{(\mu)}) - y^{(\mu)}] \nabla f(\theta, x^{(\mu)})$, and hence

$$\frac{1}{N} \sum_{\mu=1}^N \nabla \ell_{\mu} \nabla \ell_{\mu}^T = \frac{2}{N} \sum_{\mu=1}^N \ell_{\mu} \nabla f(\theta, x^{(\mu)}) \nabla f(\theta, x^{(\mu)})^T. \quad (9)$$

Now we make an approximation that ℓ_{μ} and $\nabla f(\theta, x^{(\mu)}) \nabla f(\theta, x^{(\mu)})^T$ are uncorrelated with each other. In this case, they are decoupled as

$$\begin{aligned} \frac{1}{N} \sum_{\mu=1}^N \ell_{\mu} \nabla f(\theta, x^{(\mu)}) \nabla f(\theta, x^{(\mu)})^T &\approx \left(\frac{1}{N} \sum_{\mu=1}^N \ell_{\mu} \right) \cdot \frac{1}{N} \sum_{\mu=1}^N \nabla f(\theta, x^{(\mu)}) \nabla f(\theta, x^{(\mu)})^T \\ &= L(\theta) \frac{1}{N} \sum_{\mu=1}^N \nabla f(\theta, x^{(\mu)}) \nabla f(\theta, x^{(\mu)})^T. \end{aligned} \quad (10)$$

We shall call this approximation *the decoupling approximation*, which is promising for a large network in which ∇f looks a random vector. In Sec. 5.1, we experimentally show that the decoupling approximation is a good approximation in practice for the entire training dynamics. We then obtain

$$\Sigma(\theta) \approx \frac{2L(\theta)}{NB} \sum_{\mu=1}^N \nabla f(\theta, x^{(\mu)}) \nabla f(\theta, x^{(\mu)})^T. \quad (11)$$

Equation (11) is directly related to the Hessian of the loss function near a (local or global) minimum. The Hessian is written as

$$H(\theta) = \nabla^2 L(\theta) = \frac{1}{N} \sum_{\mu=1}^N \nabla f(\theta, x^{(\mu)}) \nabla f(\theta, x^{(\mu)})^T + \frac{1}{N} \sum_{\mu=1}^N [f(\theta, x^{(\mu)}) - y^{(\mu)}] \nabla^2 f(\theta, x^{(\mu)}). \quad (12)$$

Near a minimum with a small $L(\theta)$, the last term of Eq. (12) is negligible since $|f(\theta, x^{(\mu)}) - y^{(\mu)}|$ is typically small. As a result, we obtain a simplified expression of the Hessian near a minimum θ^* :

$$H(\theta^*) \approx \frac{1}{N} \sum_{\mu=1}^N \nabla f(\theta^*, x^{(\mu)}) \nabla f(\theta^*, x^{(\mu)})^T. \quad (13)$$

Let us assume $\nabla f(\theta, x^{(\mu)}) \nabla f(\theta, x^{(\mu)})^T \approx \nabla f(\theta^*, x^{(\mu)}) \nabla f(\theta^*, x^{(\mu)})^T$ for θ within the valley of a local minimum θ^* . We then obtain by substituting Eq. (13) into Eq. (11)

$$\Sigma(\theta) \approx \frac{2L(\theta)}{B} H(\theta^*) \quad (14)$$

for θ within the valley of a local minimum θ^* .

Our formula (14) shows two important properties. First, the noise is aligned with the Hessian, which has been well known and pointed out in the literature [8, 11–13]. If the loss landscape has flat directions, which correspond to the directions of the Hessian eigenvectors belonging to vanishingly small eigenvalues, the SGD noise does not work along those directions. Consequently, SGD dynamics is frozen along those flat directions, which effectively reduces the dimension of the parameter space explored by SGD dynamics. This plays an important role in the escape efficiency. Indeed, we will see that the escape rate crucially depends on the effective dimension of a given local minimum.

Second, the noise is proportional to the loss function, which has not been pointed out and not been taken into account in the previous studies [8, 11–13] and therefore gives new insights into the SGD dynamics. Indeed, this property allows us to formulate the Langevin equation on the logarithmized loss landscape with simple additive noise as discussed in Sec. 3.2. This new formalism yields the power-law escape rate, i.e. Eqs. (22) and (27), which significantly differs from the escape rate formulae derived in Refs. [12, 13].

3.2 Logarithmized loss landscape

Let us consider the stochastic differential equation (4) with the SGD noise covariance (14), which is written as

$$d\theta_t = -\nabla L(\theta_t) dt + \sqrt{\frac{2\eta L(\theta_t)}{B} H(\theta^*)} \cdot dW_t, \quad (15)$$

where θ_t is in the valley with a local minimum θ^* . Now let us introduce the scaled time variable τ defined as

$$\tau := \int_0^t dt' L(\theta_{t'}). \quad (16)$$

Correspondingly, we introduce the Wiener process $d\tilde{W}_\tau \sim \mathcal{N}(0, I_P d\tau)$. Since $\mathcal{N}(0, I_P dt) = \mathcal{N}(0, I_P L(\theta_t) dt) = \sqrt{L(\theta_t)} \mathcal{N}(0, I_P dt)$, $d\tilde{W}_\tau$ is related to dW_t as $d\tilde{W}_\tau = \sqrt{L(\theta_t)} \cdot dW_t$. In terms of the notation $\tilde{\theta}_\tau = \theta_t$, Eq. (15) is expressed as

$$d\tilde{\theta}_\tau = -\frac{1}{L(\tilde{\theta}_\tau)} \nabla L(\tilde{\theta}_\tau) d\tau + \sqrt{\frac{2\eta H(\theta^*)}{B}} d\tilde{W}_\tau = -\left[\nabla \log L(\tilde{\theta}_\tau)\right] d\tau + \sqrt{\frac{2\eta H(\theta^*)}{B}} d\tilde{W}_\tau. \quad (17)$$

In this way, the stochastic differential equation with multiplicative noise is transformed to that with simpler additive noise. Remarkably, in Eq. (17), the gradient of $\log L$ appears. It indicates the importance of considering the landscape of $\log L$, which we call the *logarithmized loss landscape*. In the following, we use Eq. (17) to discuss the escape efficiency from local minima.

4 Escape rate from local minima

4.1 Single-variable case

We begin with a simple case in which there is a single trainable parameter ($P = 1$). In this case, by introducing the potential $U(\theta) = \log L(\theta)$ and the temperature $T = \eta h^*/B$, where $h^* := H(\theta^*)$, we can rewrite Eq. (17) as

$$d\tilde{\theta}_\tau = -U'(\tilde{\theta}_\tau) + \sqrt{2T}d\tilde{W}_\tau, \quad (18)$$

which is a type of the GLD introduced in Eq. (5) and identical to the Langevin equation of a Brownian particle coupled to a heat bath at temperature T . Similarly to Eq. (6), the steady-state distribution $\tilde{P}_{\text{ss}}(\theta)$ generated by Eq. (18) is given by the Gibbs distribution with respect to $U(\theta)$: $\tilde{P}_{\text{ss}}(\theta) \propto e^{-U(\theta)/T} \propto L(\theta)^{-B/(\eta h^*)}$. This is the distribution function of $\tilde{\theta}_\tau$ for an asymptotically large τ . However, what we really want is the stationary distribution of θ_t for an asymptotically large t . In Sec. A of Supplementary Material (SM), by using Eq. (16), we obtain the latter as

$$P_{\text{ss}}(\theta) \propto L(\theta)^{-1} \tilde{P}_{\text{ss}}(\theta) \propto L(\theta)^{-\phi}, \quad \phi = 1 + \frac{B}{\eta h^*}. \quad (19)$$

Interestingly, $P_{\text{ss}}(\theta)$ depends on $L(\theta)$ polynomially rather than exponentially as in the standard GLD [8, 24, 25]. Near a local minimum θ^* , we expand $L(\theta)$ around θ^* as $L(\theta) \approx L(\theta^*) + (h^*/2)(\theta - \theta^*)^2$. When $L(\theta^*)$ is very small, we approximately have a power-law distribution $P_{\text{ss}}(\theta) \propto (\theta - \theta^*)^{-2\phi}$. Compared with an exponential form $P(\theta) \propto e^{-L(\theta)/D}$, the power-law distribution has a long tail, which makes the escape from a local minimum more efficient.

Now we calculate the escape rate κ , which is defined as the probability per unit time of escaping from a local minimum θ^* by overcoming a saddle at θ^s , where $L'(\theta^s) = 0$ and $L''(\theta^s) < 0$. For the Langevin equation (18), the escape rate κ_τ per unit τ was obtained by Kramers [17] as

$$\kappa_\tau = \frac{1}{2\pi} \sqrt{U''(\theta^*)|U'''(\theta^s)|} e^{-\Delta U/T}, \quad (20)$$

where $\Delta U = U(\theta^s) - U(\theta^*)$ is called the potential barrier. What we want is the escape rate per unit time t . It is a reasonable assumption that θ_t stays close to θ^* for most times before escape, and hence τ is approximately given by $\tau \simeq L(\theta^*)t$. Thus the escape rate κ per unit t is given by

$$\kappa = L(\theta^*)\kappa_\tau. \quad (21)$$

By substituting Eq. (20) and $U(\theta) = \log L(\theta)$ into Eq. (21) and using $U''(\theta^c) = L''(\theta^c)/L(\theta^c)$ at θ^c satisfying $L'(\theta^c) = 0$, we obtain

$$\kappa = \frac{1}{2\pi} \sqrt{h^* |h^s|} \left[\frac{L(\theta^s)}{L(\theta^*)} \right]^{-\left(\frac{1}{2} + \frac{B}{\eta h^*}\right)}, \quad (22)$$

where $h^* = L''(\theta^*)$ and $h^s = L''(\theta^s)$. This is our escape-rate formula in the single-variable case.

4.2 Multi-variable case

Next, let us consider the multi-variable case, $\theta \in \mathbb{R}^P$ and $P > 1$. In this case, the analysis becomes involved because the SGD noise is highly anisotropic. In the over-parameterized regime ($P > N$), Eq. (13) implies that the Hessian has at least $P - N$ null eigenvalues. As we discussed in Sec. 3.1, the SGD dynamics is frozen along those flat directions, and hence SGD is restricted to an N -dimensional manifold spanned by the eigenvectors of $H(\theta^*)$ with non-zero eigenvalues. Moreover, previous studies on the Hessian spectrum have revealed that many of N non-zero eigenvalues are very small: the Hessian eigenvalues are decomposed into a bulk of near-zero eigenvalues and a small number of outliers [20, 21]. The SGD dynamics is also frozen along those almost flat directions.

Let us denote by n the number of the outliers, which is regarded as an effective dimension of the local minimum [19]. Then SGD is further restricted to the n -dimensional manifold spanned by the outlier eigenvectors $v_1, v_2, \dots, v_n \in \mathbb{R}^P$. We parameterize θ by using n parameters $z_1, z_2, \dots, z_n \in \mathbb{R}$ as

$$\theta = \theta^* + \sum_{i=1}^n z_i v_i. \quad (23)$$

The Hessian is then written as $H(\theta^*) \approx \sum_{i=1}^n h_i^* v_i v_i^T$ with the normalization $v_i^T v_j = \delta_{i,j}$.

Here, we assume that the anisotropy of the SGD noise within this n -dimensional space is not relevant, and approximate the SGD noise in Eq. (17) as an isotropic one:

$$\sqrt{\frac{2\eta H(\theta^*)}{B}} d\tilde{W}_\tau \approx \sqrt{\frac{2\eta h^*}{B}} d\tilde{W}_\tau, \quad (24)$$

where $h^* \in \mathbb{R}^+$ characterizes the magnitude of the Hessian outliers. This assumption is completely justified when the loss landscape is isotropic within the n -dimensional subspace near the minimum. Even if the Hessian at the minimum is not isotropic, the approximation (24) is justified when the directions of the Hessian eigenvectors do not change within the valley. In the latter case, the escape path is a straight line along the direction of a Hessian eigenvector v_e , where $e \in \{1, 2, \dots, n\}$ identifies the escape direction, and h^* corresponds to the Hessian eigenvalue at the minimum along the escape direction, i.e. $h^* = h_e^*$. See Sec. B of SM for the details.

Under these approximations, i.e. the restriction to the n -dimensional subspace with Eq. (23) and the isotropic-noise approximation (24), Eq. (17) becomes

$$dz_\tau = -(\nabla_z \log L) d\tau + \sqrt{\frac{2\eta h^*}{B}} d\tilde{W}_\tau. \quad (25)$$

The quasi-stationary distribution $P_{ss}(\theta)$ within the valley including the local minimum $\theta = \theta^*$ (i.e. $z = 0$) is again given by Eq. (19): $P_{ss}(\theta) \propto L(\theta)^{-\phi}$ with $\phi = 1 + B/(\eta h^*)$.

Since Eq. (25) is equivalent to the Brownian motion at temperature $T = \eta h^*/B$ under the potential energy $U(\theta) = \log L(\theta)$, we can use the escape-rate formula derived in physics [18]. According to it, the escape rate κ_τ per unit τ is given by

$$\kappa_\tau = \frac{|u_e^s|}{2\pi} \sqrt{\frac{\det \nabla_z^2 U(\theta^*)}{|\det \nabla_z^2 U(\theta^s)|}} e^{-\Delta U/T}, \quad (26)$$

where u_e^s is the negative eigenvalue of $\nabla_z^2 U(\theta^s)$ corresponding to the escape direction. Again we transform τ to t by using $\tau \approx L(\theta^*)t$, and obtain the escape rate κ per time t as

$$\kappa = L(\theta^*)\kappa_\tau = \frac{|h_e^s|}{2\pi} \sqrt{\frac{\det \hat{H}(\theta^*)}{|\det \hat{H}(\theta^s)|}} \left[\frac{L(\theta^s)}{L(\theta^*)} \right]^{-\left(\frac{B}{\eta h^*} + 1 - \frac{n}{2}\right)}, \quad (27)$$

where $\hat{H}(\theta) = \nabla_z^2 L(\theta)$ is the Hessian restricted to the n -dimensional manifold spanned by v_1, v_2, \dots, v_n , and $h_e^s = u_e^s L(\theta^s)$ is the negative eigenvalue of $\hat{H}(\theta^s)$ corresponding to the escape direction.² This is our primary result.

The factor $[L(\theta^s)/L(\theta^*)]^{-\left(\frac{B}{\eta h^*} + 1 - \frac{n}{2}\right)}$ increases with h^* and n , which indicates that sharp minima (i.e. minima with large h^*) or minima with large n are unstable. This fact explains why SGD finds flat minima with a low effective dimension n . Equation (27) also implies that the effective dimension of any stable minima must satisfy

$$n < 2 \left(\frac{B}{\eta h^*} + 1 \right). \quad (28)$$

The dependence of the escape rate on the effective dimension is a new insight that is naturally explained by the picture of the logarithmized loss landscape. It arises from the ratio of the determinants of the logarithmized-loss Hessian: $\det \nabla_z^2 U(\theta^*)/|\det \nabla_z^2 U(\theta^s)| = [\det \hat{H}(\theta^*)/|\det \hat{H}(\theta^s)|] \cdot [L(\theta^s)/L(\theta^*)]^{n/2}$.

Our escape rate formula (27) depends polynomially on the ratio of the losses at a minimum and a saddle, rather than exponentially on the difference of the two as in formulae derived in the previous works [11–13]. This difference is due to the fact that the inhomogeneity of the SGD noise strength is not taken into account in the previous studies [12, 13]. According to our escape rate formula, even if the loss barrier height ΔL

²If eigenvalues of $\hat{H}(\theta^*)$ and those of $\hat{H}(\theta^s)$ coincide with each other except for the escape direction e , $\det \hat{H}(\theta^*)/\det \hat{H}(\theta^s) = h_e^*/h_e^s$ holds, and Eq. (27) is simplified as $\kappa = (1/2\pi)\sqrt{h_e^*/h_e^s}[L(\theta^s)/L(\theta^*)]^{-\left(\frac{B}{\eta h^*} + 1 - \frac{n}{2}\right)}$.

is the same, minima with smaller values of $L(\theta^*)$ are more stable than those with larger values of $L(\theta^*)$. In particular, a global minimum with zero training loss, which is realized in an overparameterized regime [26], is absolutely stable since $U(\theta^*) = \log L(\theta^*) = -\infty$, i.e. the well in the logarithmized loss landscape is infinitely deep.

5 Experiments

Our key theoretical observation is that the SGD noise strength is proportional to the loss function, which is obtained as a result of the decoupling approximation, i.e. Eq. (10). This property leads us to the Langevin equation (17) with the logarithmized loss gradient and an additive noise through application of a non-uniform time transformation of Eq. (16). Equation (17) implies the stationary distribution (19) and the escape rate (27).

In Sec. 5.1, we show that the decoupling approximation is valid during entire training dynamics. In Sec. 5.2, we measure the SGD noise strength and confirm that it is indeed proportional to the loss function near a minimum. In Sec. 5.3, in the linear regression problem, we experimentally test the validity of Eq. (19) for the stationary distribution and Eq. (27) for the escape rate.

5.1 Experimental verification of the decoupling approximation

Let us compare the eigenvalue distribution of the exact matrix given by the left-hand side of Eq. (10) with that of the decoupled one given by the right-hand side. We consider a binary classification problem using the first 10^4 samples of the MNIST dataset such that we classify each image into even (its label is $y = +1$) or odd number (its label is $y = -1$). The network has two hidden layers, each of which has 100 units and the ReLU activation, followed by the output layer of a single unit with no activation. Starting from the Glorot initialization, the training is performed via SGD with the mean-square loss, where we fix $\eta = 0.01$ and $B = 100$.

Figure 1 shows histograms of their eigenvalues at different stages of the training: (a) at initialization, (b) after 50 epochs, and (c) after 500 epochs. We see that the exact matrix and the approximate one have statistically similar eigenvalue distributions except for very small eigenvalues during training dynamics. This means that the decoupling approximation always holds during training.

5.2 Measurements of the SGD noise strength

As a measure of the SGD noise strength, let us consider the norm of the noise vector ξ given by

$$\langle \xi^T \xi \rangle = \text{Tr} \Sigma = \frac{1}{B} \frac{N - B}{N - 1} \mathcal{N}, \quad \mathcal{N} := \frac{1}{N} \sum_{\mu=1}^N \nabla \ell_{\mu}^T \nabla \ell_{\mu} - \nabla L^T \nabla L. \quad (29)$$

Here we present experimental results for two architectures and datasets. First, we consider training of the Fashion-MNIST dataset by using a fully connected neural network

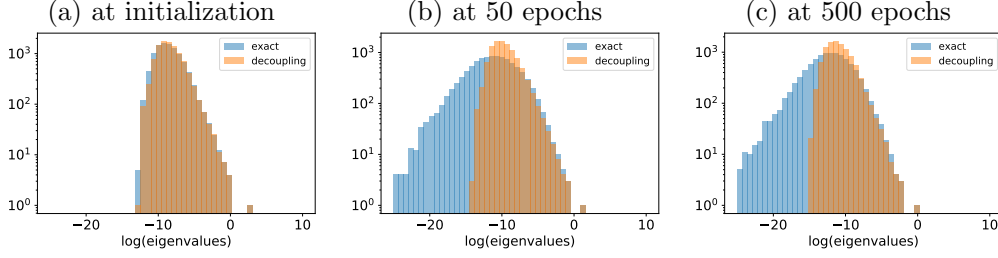


Figure 1: Comparison of the eigenvalue distributions of the left-hand side (exact expression) and the right-hand side (decoupled one) of Eq. (12) in the main text. They agree with each other except for very small eigenvalues during entire training dynamics.

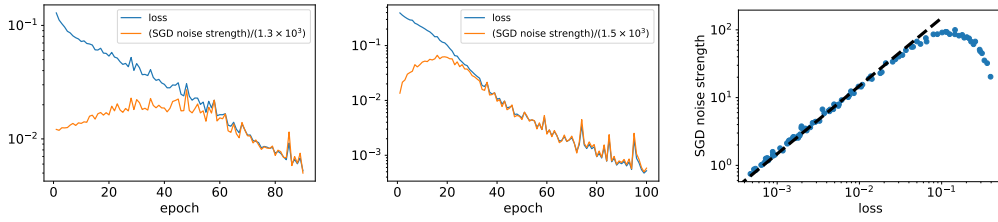


Figure 2: Training dynamics of the loss function and the SGD noise strength \mathcal{N} . In the figure, we multiplied \mathcal{N} by a numerical factor to emphasize that \mathcal{N} is actually proportional to the loss in a later stage of the training. (Left) Fully-connected network trained by the Fashion-MNIST dataset. (Middle) Convolutional network trained by the CIFAR-10 dataset. (Right) the loss vs \mathcal{N} in the training of the convolutional network. The dashed line is a straight line of slope 1, which implies $\mathcal{N} \propto L(\theta)$.

with three hidden layers, each of which has 2×10^3 units and the ReLU activation, followed by the output layer of 10 units with no activation (classification labels are given in the one-hot representation). Second, we consider training of the CIFAR-10 dataset by using a convolutional neural network. Following Keskar *et al.* [15], let us denote a stack of n convolutional layers of a filters and a kernel size of $b \times c$ with the stride length of d by $n \times [a, b, c, d]$. We use the configuration: $3 \times [64, 3, 3, 1]$, $3 \times [128, 3, 3, 1]$, $3 \times [256, 3, 3, 1]$, where a MaxPool(2) is applied after each stack. To all layers, the ReLU activation is applied. Finally, an output layer consists of 10 units with no activation.

Starting from the Glorot initialization, the network is trained by SGD of the mini-batch size $B = 100$ and $\eta = 0.1$ for the mean-square loss. During the training, we measure the training loss and the noise strength \mathcal{N} for every epoch. Numerical results are given in Fig. 2. We see that roughly $\mathcal{N} \propto L$ at a later stage of the training, which agrees with our theoretical prediction.

Although \mathcal{N} is not proportional to L at an early stage of the training, it does not

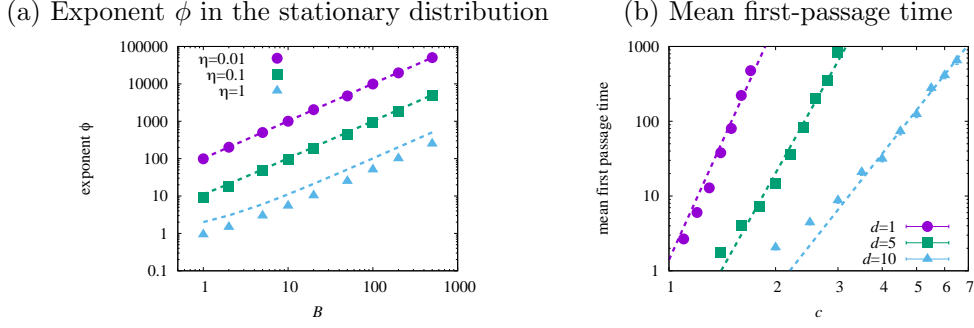


Figure 3: (a) Exponent ϕ for the stationary distribution $P_{\text{ss}}(\theta) \propto L(\theta)^{-\phi}$ for $d = 1$. Dashed lines show theoretical values $\phi = 1 + B/(\eta h^*)$. (b) Log-log plot of the mean first-passage time t_p vs $c = L(\theta^s)/L(\theta^*)$ for $B = 1$ and $\eta = 0.1$. Error bars are smaller than the symbols. Dashed lines show theoretical prediction, $t_p \propto \kappa^{-1} \propto c^{\phi-n/2}$ with $n = d$.

mean that Eq. (11) is invalid there. Since the decoupling approximation is valid for the entire training dynamics, Eq. (11) always holds. The reason why the SGD noise strength does not decrease with the loss function in the early-stage dynamics is that $\mathcal{N} \approx 2L(\theta) \times (1/N) \sum_{\mu=1}^N \nabla f(\theta, x^{(\mu)})^T \nabla f(\theta, x^{(\mu)})$, but the quantity $(1/N) \sum_{\mu=1}^N \nabla f(\theta, x^{(\mu)})^T \nabla f(\theta, x^{(\mu)})$ also changes during training.

Although Eq. (11) is derived for the mean-square loss, the relation $\mathcal{N} \propto L(\theta)$ holds in more general loss functions; see Sec. C of SM for general argument and experiments on the cross entropy loss.

5.3 Experimental test of stationary distribution and escape rate formula

We experimentally verify our theoretical predictions in the linear regression problem. Let us consider the training dataset $\mathcal{D} = \{(x^{(\mu)}, y^{(\mu)}) : \mu = 1, 2, \dots, N\}$, where each entry of $x^{(\mu)} \in \mathbb{R}^d$ and its label $y^{(\mu)} \in \mathbb{R}$ are i.i.d. Gaussian random variables of zero mean and unit variance. The output for an input x is given by $f(\theta, x) = \theta^T x$, where $\theta \in \mathbb{R}^d$ is the trainable network parameter. We focus on the case of $d \ll N$, where the training loss remains finite even at the global minimum. We optimize θ via SGD. The mean-square loss $L(\theta) = (1/2N) \sum_{\mu=1}^N (\theta x^{(\mu)} - y^{(\mu)})^2$ is quadratic and has a unique minimum at $\theta \approx 0$.

First, we test Eq. (19), i.e. the stationary distribution, for $d = 1$ and $N = 10^5$. We sampled the value of θ_k at every 100 iterations ($k = j \times 100$, $j = 1, 2, \dots, 10^4$) and made a histogram. We then fit the histogram to the form $P_{\text{ss}}(\theta) \propto L(\theta)^{-\phi}$ and determine the exponent ϕ . Our theory predicts $\phi = 1 + B/(\eta h^*)$. Numerical results for the exponent ϕ are presented in Fig. 3 (a) against B for three fixed learning rates η . In the same figure, theoretical values of ϕ are plotted in dashed lines. The agreement between theory and experiment is fairly well. For a large learning rate $\eta = 1$, the exponent slightly deviates from its theoretical value. This is due to the effect of a finite learning rate (recall that η

is assumed to be small in deriving the continuous-time stochastic differential equation).

Next, we test our formula on the escape rate, Eq. (27). Although the mean-square loss is quadratic and no barrier crossing occurs, we can measure the first passage time, which imitates the escape time for a non-convex loss landscape. Let us fix a threshold value of the loss function. The first passage time t_p is defined as the shortest time at which the loss exceeds the threshold value. Here, time t is identified as ηk , where k denotes the number of iterations in discrete SGD (2). We identify the threshold value as $L(\theta^s)$, i.e., the loss at the saddle in the escape problem. It is expected that t_p is similar to the escape time and proportional to κ^{-1} .

The Hessian $H = (1/N) \sum_{\mu=1}^N x^{(\mu)} x^{(\mu)\top}$ has d nonzero eigenvalues, all of which are close to unity. We can therefore identify $h^* = 1$ and $n = d$. The mean first passage time over 100 independent runs is measured for varying threshold values which are specified by $c = L(\theta^s)/L(\theta^*) > 1$. Experimental results for $N = 10^4$ are presented in Fig. 3 (b). Dashed straight lines have slope $B/(\eta h^*) + 1 - n/2$. Experiments show that the first passage time behaves as $t_p \propto [L(\theta^s)/L(\theta^*)]^{B/(\eta h^*) + 1 - n/2}$, which agrees with our theoretical evaluation of κ^{-1} [see Eq. (27)]. We conclude that the escape rate crucially depends on the effective dimension n , which is not explained by the previous results [11–14].

6 Conclusion

In this work, we have shown that the SGD noise strength for the mean-square loss is proportional to the loss function near a minimum, i.e. Eq. (14), and we have used it to derive the stochastic differential equation (17) with additive noise near a minimum via a non-uniform time transformation (16). The original multiplicative noise is reduced to simpler additive noise, but instead the gradient of the loss function is replaced by that of the logarithmized loss function $U(\theta) = \log L(\theta)$. This stochastic differential equation has a power-law stationary distribution near a minimum (19), which is confirmed in experiments. This new formalism yields the power-law escape rate formula (27) whose exponent depends on η , B , h^* , and n , which has never been proposed in previous works. Our escape-rate formula explains an empirical fact that SGD favors flat minima with low effective dimensions.

Our simple formula (14) on the SGD-noise covariance has not been reported previously. It is derived by the decoupling approximation, whose validity is confirmed experimentally. This formula as well as our new formalism of the Langevin equation on the logarithmized loss landscape should help understand more deeply the SGD dynamics in machine learning problems.

References

- [1] A. Krizhevsky, I. Sutskever, and G. E. Hinton, Imagenet classification with deep convolutional neural networks, in *Advances in Neural Information Processing Systems* (2012) pp. 1097–1105.

- [2] Y. LeCun, Y. Bengio, and G. Hinton, Deep learning, *Nature* **521**, 436–444 (2015).
- [3] G. Hinton, L. Deng, D. Yu, G. E. Dahl, A.-r. Mohamed, N. Jaitly, A. Senior, V. Vanhoucke, P. Nguyen, T. N. Sainath, and Others, Deep neural networks for acoustic modeling in speech recognition: The shared views of four research groups, *IEEE Signal processing magazine* **29**, 82–97 (2012).
- [4] R. Collobert and J. Weston, A unified architecture for natural language processing: Deep neural networks with multitask learning, in *International Conference on Machine Learning* (2008).
- [5] R. Iten, T. Metger, H. Wilming, L. Del Rio, and R. Renner, Discovering Physical Concepts with Neural Networks, *Physical Review Letters* **124**, 10508 (2020), [arXiv:1807.10300](#).
- [6] V. Bapst, T. Keck, A. Grabska-Barwińska, C. Donner, E. D. Cubuk, S. S. Schoenholz, A. Obika, A. W. Nelson, T. Back, D. Hassabis, and P. Kohli, Unveiling the predictive power of static structure in glassy systems, *Nature Physics* **16**, 448–454 (2020).
- [7] A. Seif, M. Hafezi, and C. Jarzynski, Machine learning the thermodynamic arrow of time, *Nature Physics* **17**, 105–113 (2021), [arXiv:1909.12380](#).
- [8] S. Jastrzębski, Z. Kenton, D. Arpit, N. Ballas, A. Fischer, Y. Bengio, and A. Storkey, Three Factors Influencing Minima in SGD, [arXiv:1711.04623](#).
- [9] L. Wu, C. Ma, and E. Weinan, How SGD selects the global minima in over-parameterized learning: A dynamical stability perspective, in *Advances in Neural Information Processing Systems* (2018).
- [10] J. Wu, W. Hu, H. Xiong, J. Huan, V. Braverman, and Z. Zhu, On the Noisy Gradient Descent that Generalizes as SGD, in *International Conference on Machine Learning* (2020) [arXiv:1906.07405](#).
- [11] Z. Zhu, J. Wu, B. Yu, L. Wu, and J. Ma, The anisotropic noise in stochastic gradient descent: Its behavior of escaping from sharp minima and regularization effects, in *International Conference on Machine Learning* (2019) [arXiv:1803.00195](#).
- [12] Z. Xie, I. Sato, and M. Sugiyama, A Diffusion Theory For Deep Learning Dynamics: Stochastic Gradient Descent Exponentially Favors Flat Minima, in *International Conference on Learning Representations* (2021) [arXiv:2002.03495](#).
- [13] K. Liu, L. Ziyin, and M. Ueda, Noise and Fluctuation of Finite Learning Rate Stochastic Gradient Descent, [arXiv:arXiv:2012.03636v3](#).
- [14] Q. Meng, S. Gong, W. Chen, Z. M. Ma, and T. Y. Liu, Dynamic of Stochastic Gradient Descent with State-Dependent Noise, [arXiv:2006.13719](#).

- [15] N. S. Keskar, J. Nocedal, P. T. P. Tang, D. Mudigere, and M. Smelyanskiy, On large-batch training for deep learning: Generalization gap and sharp minima, in *International Conference on Learning Representations* (2017) [arXiv:1609.04836](#).
- [16] E. Hoffer, I. Hubara, and D. Soudry, Train longer, generalize better: closing the generalization gap in large batch training of neural networks, in *Advances in Neural Information Processing Systems* (2017) [arXiv:1705.08741](#).
- [17] H. A. Kramers, Brownian motion in a field of force and the diffusion model of chemical reactions, *Physica* **7**, 284–304 (1940).
- [18] J. S. Langer, Statistical theory of the decay of metastable states, *Annals of Physics* **54**, 258–275 (1969).
- [19] D. MacKay, Bayesian model comparison and backprop nets, in *Advances in Neural Information Processing Systems* (1992).
- [20] L. Sagun, U. Evci, V. U. Güney, Y. Dauphin, and L. Bottou, Empirical analysis of the hessian of over-parametrized neural networks, [arXiv:1706.04454](#).
- [21] V. Pappayan, Measurements of three-level hierarchical structure in the outliers in the spectrum of deepnet Hessians, in *International Conference on Machine Learning* (2019) [arXiv:1901.08244](#).
- [22] Q. Li, C. Tai, and E. Weinan, Stochastic modified equations and adaptive stochastic gradient algorithms, in *International Conference on Machine Learning* (2017) [arXiv:1511.06251](#).
- [23] S. L. Smith and Q. V. Le, A Bayesian perspective on generalization and stochastic gradient descent, in *International Conference on Learning Representations* (2018) [arXiv:1710.06451](#).
- [24] I. Sato and H. Nakagawa, Approximation analysis of stochastic gradient Langevin dynamics by using fokker-planck equation and ito process, in *International Conference on Machine Learning* (2014).
- [25] Y. Zhang, P. Liang, and M. Charikar, A hitting time analysis of stochastic gradient Langevin dynamics, in *Proceedings of Machine Learning Research* (2017) [arXiv:1702.05575](#).
- [26] C. Zhang, S. Bengio, M. Hardt, B. Recht, and O. Vinyals, Understanding Deep Learning Requires Rethinking of Generalization, in *International Conference on Learning Representations* (2017).

Supplementary Material

A. Stationary distribution

Since $\tilde{\theta}_\tau$ obeys a simple Langevin equation

$$d\tilde{\theta}_\tau = -U'(\tilde{\theta}_\tau) + \sqrt{2T}d\tilde{W}_\tau, \quad (\text{S1})$$

the stationary distribution of $\tilde{\theta}_\tau$ is given by the Gibbs distribution $\tilde{P}_{\text{ss}}(\theta) \propto e^{-U(\theta)/T}$. On the other hand, what we want is the stationary distribution $P_{\text{ss}}(\theta)$ of θ_t , where $\theta_t = \tilde{\theta}_\tau$ with $\tau = \int_0^t dt' L(\theta_{t'})$. In this section, we show the relation between the two distributions: $P_{\text{ss}}(\theta) \propto L(\theta)^{-1} \tilde{P}_{\text{ss}}(\theta)$.

We express the stationary distributions in terms of the long-time average of the delta function:

$$P_{\text{ss}}(\theta) = \lim_{s \rightarrow \infty} \frac{1}{s} \int_0^s dt \delta(\theta_t - \theta), \quad \tilde{P}_{\text{ss}}(\theta) = \lim_{s \rightarrow \infty} \frac{1}{s} \int_0^s d\tau \delta(\tilde{\theta}_\tau - \theta). \quad (\text{S2})$$

By using the relation $\tau = \int_0^t dt' L(\theta_{t'})$, we have $d\tau = L(\theta_t)dt$. For a sufficiently large t , we also obtain $\tau \sim t\bar{L}$, where $\bar{L} := \lim_{s \rightarrow \infty} (1/s) \int_0^s dt' L(\theta_{t'})$ denotes the long-time average of $L(\theta_t)$. By using them, $P_{\text{ss}}(\theta)$ is rewritten as

$$\begin{aligned} P_{\text{ss}}(\theta) &\approx \lim_{s \rightarrow \infty} \frac{1}{s} \int_0^{s\bar{L}} d\tau \frac{\delta(\tilde{\theta}_\tau - \theta)}{L(\tilde{\theta}_\tau)} \\ &= \frac{1}{L(\theta)} \lim_{s \rightarrow \infty} \frac{\bar{L}}{s\bar{L}} \int_0^{s\bar{L}} d\tau \delta(\tilde{\theta}_\tau - \theta) \\ &= \frac{\bar{L}}{L(\theta)} \tilde{P}_{\text{ss}}(\theta). \end{aligned} \quad (\text{S3})$$

We thus obtain the desired relation, $P_{\text{ss}}(\theta) \propto L(\theta)^{-1} \tilde{P}_{\text{ss}}(\theta)$.

B. Justification of the isotropic-noise approximation within the n -dimensional subspace

We now show that the isotropic-noise approximation is valid when the directions of the eigenvectors of the Hessian do not change within the valley of a given local minimum. In this case, $\partial^2 U / \partial z_i \partial z_j = 0$ for any $i \neq j$, where the Hessian at the minimum is given by $H(\theta^*) \approx \sum_{i=1}^n h_i^* v_i v_i^T$ (h_i is an eigenvalue and v_i is the corresponding eigenvector of $H(\theta^*)$) and the displacement vector $z \in \mathbb{R}^n$ is defined by $\theta = \theta^* + \sum_{i=1}^n z_i v_i$. The stochastic differential equation $dz = -\nabla_z U d\tau + \sqrt{2\eta H(\theta^*)/B} d\tilde{W}_\tau$ is then equivalent to the following Fokker-Planck equation for the distribution function $P(z, \tau)$ of z at τ :

$$\frac{\partial P(z, \tau)}{\partial \tau} = \sum_{i=1}^n \left[\frac{\partial}{\partial z_i} \left(\frac{\partial U}{\partial z_i} P \right) + \frac{\eta h_i^*}{B} \frac{\partial^2}{\partial z_i^2} P \right]. \quad (\text{S4})$$

Let us assume that the direction of e th eigenvector v_e corresponds to the escape direction. We denote by $z_\perp \in \mathbb{R}^{n-1}$ the displacement perpendicular to the escape direction, and write $z = (z_e, z_\perp)$. At the saddle z^s , $\nabla_z U(z^s) = 0$, $h_e^s < 0$ and $h_i^s > 0$ for all $i \neq e$, where $\{h_i^s\}$ is the set of eigenvalues of the Hessian at z^s .

Under the above setting, we derive the escape rate formula following Kramers [S1]. The steady current $J \in \mathbb{R}^n$ is aligned to the escape direction, and hence $J_e \neq 0$ and $J_\perp = 0$. Let us denote by P^* the total probability within the valley of a given minimum θ^* and by \mathcal{J} the total current flowing to outside of the valley through the saddle $\theta^s = \theta^* + z^s$. It is assumed that \mathcal{J} is small and P^* is almost stationary. The escape rate κ_τ is then given by

$$\kappa_\tau = \frac{\mathcal{J}}{P^*}. \quad (\text{S5})$$

The escape rate κ per unit time is given by

$$\kappa = L(\theta^*) \kappa_\tau = L(\theta^*) \frac{\mathcal{J}}{P^*}. \quad (\text{S6})$$

We now evaluate P^* and \mathcal{J} . To evaluate P^* , it is necessary to know about the stationary distribution near the minimum θ^* . Near the minimum θ^* (i.e. small z),

$$U(\theta) = \log L(\theta) \approx U(\theta^*) + \frac{(\theta - \theta^*)^T H(\theta^*) (\theta - \theta^*)}{2L(\theta^*)} = U(\theta^*) + \frac{z^T H(\theta^*) z}{2L(\theta^*)} \quad (\text{S7})$$

and

$$\frac{\partial U}{\partial z_i} \approx \frac{1}{L(\theta^*)} \sum_{j=1}^n H_{ij}^* z_j, \quad (\text{S8})$$

where $H^* = H(\theta^*)$. By substituting it into the Fokker-Planck equation (S4), we obtain

$$\frac{\partial P(z, \tau)}{\partial \tau} = \sum_{i=1}^n \frac{\partial}{\partial z_i} \left[\sum_{j=1}^n H_{ij}^* \left(\frac{z_j}{L(\theta^*)} + \frac{\eta}{B} \frac{\partial}{\partial z_j} \right) P \right]. \quad (\text{S9})$$

If for all j ,

$$\left(\frac{z_j}{L(\theta^*)} + \frac{\eta}{B} \frac{\partial}{\partial z_j} \right) P_{\text{ss}}(z), \quad (\text{S10})$$

$P_{\text{ss}}(z)$ is the stationary distribution near the minimum θ^* . Indeed,

$$P_{\text{ss}}(z) = P(\theta^*) e^{-\frac{B}{2\eta L(\theta^*)} \sum_{i=1}^n z_i^2} \quad (\text{S11})$$

satisfies this condition. It should be noted that the stationary distribution is independent of the Hessian eigenvalues $\{h_i^*\}$. By using Eq. (S11), P^* is evaluated as

$$P^* \approx \int dz_1 dz_2 \dots dz_n P_{\text{ss}}(z) = P(\theta^*) \left[\frac{2\eta L(\theta^*)}{B} \right]^{n/2}. \quad (\text{S12})$$

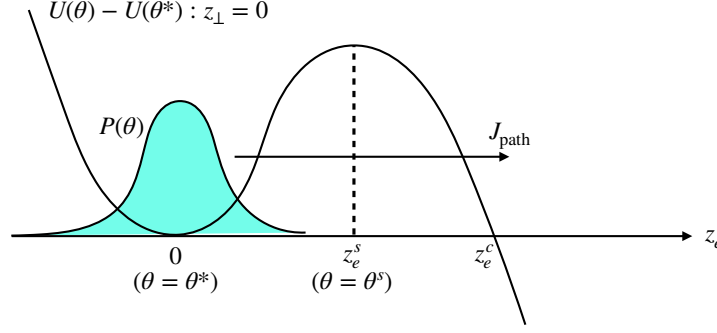


Figure S1: Illustrative picture of the escape from the potential barrier.

Next, let us evaluate \mathcal{J} . The probability current J along the escape direction e is given by

$$J_e = -\frac{\partial U}{\partial z_e} P - \frac{\eta h_e^*}{B} \frac{\partial}{\partial z_e} P. \quad (\text{S13})$$

At the saddle, the current vector J_\perp perpendicular to the escape direction is zero, and hence the probability distribution near the saddle with $z_e = z_e^s$ and $z_\perp \neq 0$ is also evaluated in a similar way as in Eq. (S11):

$$P(z_e = z_e^s, z_\perp) \approx P(z_e = z_e^s, z_\perp = 0) e^{-\frac{B}{2\eta L(\theta^s)} z_\perp^2}. \quad (\text{S14})$$

By substituting it into Eq. (S13), we obtain

$$J_e(z_e^s, z_\perp) = J_{\text{path}} e^{-\frac{B}{2\eta L(\theta^s)} z_\perp^2}, \quad (\text{S15})$$

where the current along the escape path ($z_\perp = 0$) is denoted by $J_{\text{path}} := J(z_e^s, z_\perp = 0)$. The total current through the saddle is then evaluated as

$$\mathcal{J} = \int dz_\perp J_e(z_e^s, z_\perp) = J_{\text{path}} \left[\frac{2\pi\eta L(\theta^s)}{B} \right]^{(n-1)/2}. \quad (\text{S16})$$

When the distribution function is almost stationary, Eq. (S4) yields $\partial J_e(z_e, z_\perp = 0)/\partial z_e \approx 0$, and hence the current along the escape path is approximately constant $J_e(z_e, z_\perp = 0) \approx J_{\text{path}}$. Since $J_e(z_e, z_\perp = 0)$ is given by Eq. (S13) by putting $z_\perp = 0$, we have

$$J_{\text{path}} = -\left. \frac{\partial U}{\partial z_e} \right|_{z_\perp=0} P - \frac{\eta h_e^*}{B} \frac{\partial P}{\partial z_e} = -\frac{\eta h_e^*}{B} e^{-\frac{B}{\eta h_e^*} U} \frac{\partial}{\partial z_e} \left(e^{\frac{B}{\eta h_e^*} U} P \right). \quad (\text{S17})$$

By multiplying $e^{\frac{B}{\eta h_e^*} U}$ in both sides and integrating over z_e from 0 to z_e^c , where z_e^c defined as $U(\theta^* + z_e^c v_e) = U(\theta^*)$ (see Fig. S1), we obtain

$$J_{\text{path}} \int_0^{z_e^c} dz_e e^{\frac{B}{\eta h_e^*} U} = \frac{\eta h_e^*}{B} e^{\frac{B}{\eta h_e^*} U(\theta^*)} P(\theta^*), \quad (\text{S18})$$

where it is assumed that the probability at z_e^c is small and negligible, $P(z_e = z_e^c, z_\perp = 0) \approx 0$. By using the saddle-point method, the integral in the left-hand side of Eq. (S18) is evaluated as

$$\begin{aligned} \int_0^{z_e^c} dz_e e^{\frac{B}{\eta h_e^*} U} &\approx \int_{-\infty}^{\infty} dz_e \exp \left[\frac{B}{\eta h_e^*} \left(U(\theta^s) + \frac{h_e^s}{2L(\theta^s)} (z_e - z_e^s)^2 \right) \right] \\ &= \left(\frac{2\pi\eta h_e^*}{B|h_e^s|L(\theta^s)} \right)^{1/2} e^{\frac{B}{\eta h_e^*} U(\theta^s)}. \end{aligned} \quad (\text{S19})$$

By plugging it into Eq. (S18), we obtain

$$J_{\text{path}} = \left(\frac{\eta h_e^* |h_e^s|}{2\pi B L(\theta^s)} \right)^{1/2} e^{-\frac{B}{\eta h_e^*} \Delta U} P(\theta^*), \quad (\text{S20})$$

where $\Delta U = U(\theta^s) - U(\theta^*)$. The total current \mathcal{J} in Eq. (S16) is then expressed as

$$\mathcal{J} = \frac{\sqrt{h_e^* |h_e^s|}}{2\pi L(\theta^s)} \left(\frac{2\pi\eta L(\theta^s)}{B} \right)^{n/2} e^{-\frac{B}{\eta h_e^*} \Delta U} P(\theta^*). \quad (\text{S21})$$

By using Eqs. (S12) and (S21), the escape rate κ in Eq. (S6) is evaluated as

$$\kappa = L(\theta^*) \frac{\mathcal{J}}{P^*} = \frac{\sqrt{h_e^* |h_e^s|}}{2\pi} \left[\frac{L(\theta^s)}{L(\theta^*)} \right]^{\frac{n}{2}-1} e^{-\frac{B}{\eta h_e^*} \Delta U}. \quad (\text{S22})$$

Since $\Delta U = \log[L(\theta^s)/L(\theta^*)]$, we finally obtain

$$\kappa = \frac{\sqrt{h_e^* |h_e^s|}}{2\pi} \left[\frac{L(\theta^s)}{L(\theta^*)} \right]^{-\left(\frac{B}{\eta h_e^*} + 1 - \frac{n}{2}\right)}, \quad (\text{S23})$$

which is exactly identical to the escape rate formula derived in the main text using the isotropic-noise approximation with $h^* = h_e^*$.

In this way, the isotropic-noise approximation is justified even when the loss landscape is not isotropic near the minimum. We have assumed that the directions of the eigenvectors of the Hessian do not change within the valley of a given local minimum. Under this assumption, the Fokker-Planck equation along the escape path is decoupled from the perpendicular directions z_\perp . Moreover, we have seen that the stationary distribution near a minimum is independent of the Hessian eigenvalues. These properties explain the reason why the isotropic-noise approximation is justified in this case.

C. Other loss functions

In our paper, we mainly focus on the mean-square loss, for which we can analytically derive the relation between the loss $L(\theta)$ and the SGD noise covariance $\Sigma(\theta)$. An important observation is that the SGD noise strength \mathcal{N} is proportional to the loss, i.e., $\mathcal{N} \propto L(\theta)$ (see Sec. 5.2 of the main text for the definition of \mathcal{N}).

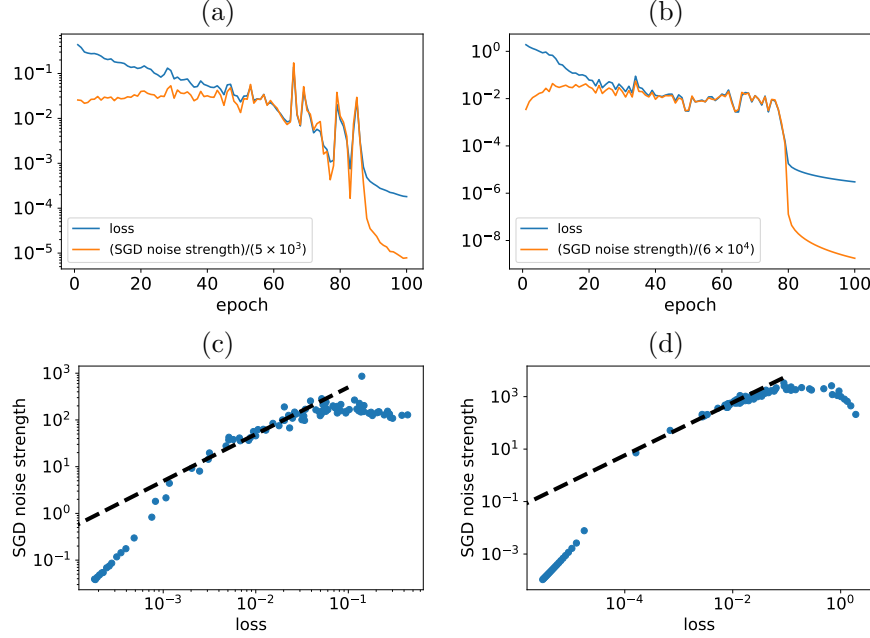


Figure S2: Training dynamics of the loss function and the SGD noise strength \mathcal{N} for (a) a fully connected network trained by the Fashion-MNIST dataset and (b) a convolutional network trained by the CIFAR-10 dataset. In the figure, we multiplied \mathcal{N} by a numerical factor to emphasize that \mathcal{N} is actually proportional to the loss in an intermediate stage of the training. Loss vs \mathcal{N} for (c) a fully connected network trained by the Fashion-MNIST and (d) a convolutional network trained by CIFAR-10. Dashed lines in (c) and (d) are straight lines of slope 1, which imply $\mathcal{N} \propto L(\theta)$.

Here, we argue that the relation $\mathcal{N} \propto L(\theta)$ also holds in more general situations. During the training, the value of ℓ_μ will fluctuate from sample to sample. At a certain time step of SGD, let us suppose that $N - M$ samples in the training dataset are already classified correctly and hence $\ell_\mu \sim 0$, whereas the other M samples are not and hence $\ell_\mu \sim 1$. The loss function is then given by $L(\theta) = (1/N) \sum_{\mu=1}^N \ell_\mu \sim M/N$. When ℓ_μ is small, $\nabla \ell_\mu$ will also be small. Therefore, for $N - M$ samples with $\ell_\mu \sim 0$, $\nabla \ell_\mu \sim 0$ also holds. The other M samples will have non-small gradients: $\|\nabla \ell_\mu\|^2 \sim g$, where $g > 0$ is a certain positive constant. We thus estimate \mathcal{N} as $\mathcal{N} \approx (1/N) \sum_{\mu=1}^N \nabla \ell_\mu^T \nabla \ell_\mu \sim gM/N \sim gL(\theta)$. In this way, $\mathcal{N} \propto L(\theta)$ will hold, irrespective of the loss function.

However, we emphasize that this is a crude argument. In particular, the above argument will not hold near a global minimum because all the samples are correctly classified there, which implies that ℓ_μ is small for all μ , in contrast to the above argument relying on the existence of M wrongly classified samples with $\ell_\mu \sim 1$ and $\|\nabla \ell_\mu\|^2 \sim g$.

We now experimentally test the relation $\mathcal{N} \propto L(\theta)$ for the cross-entropy loss. We

consider the same architectures and datasets in Sec. 5.2 of the main text: a fully connected neural network trained by Fashion-MNIST and a convolutional neural network trained by CIFAR-10 (see Sec. 5.2 for the detail). We fix $B = 100$ in both cases, and $\eta = 0.1$ for the fully connected network and $\eta = 0.05$ for the convolutional network. Experimental results are presented in Fig. S2. We find that the relation $\mathcal{N} \propto L(\theta)$ seems true at an intermediate stage of the training dynamics, although the proportionality is less clear compared with Fig. 2 in the main text for the mean-square loss.

We also find that for sufficiently small values of the loss, $\mathcal{N} \propto L(\theta)^2$ [see Fig. S2 (c) and (d)], whose implications should be pursued in future studies.

References

- [S1] H. A. Kramers, Brownian motion in a field of force and the diffusion model of chemical reactions, *Physica* **7**, 284–304 (1940).